ACS Medicinal Chemistry Letters

Letter

LpxC Inhibitors: Design, Synthesis, and Biological Evaluation of Oxazolidinones as Gram-negative Antibacterial Agents

Haruaki Kurasaki, Kosuke Tsuda, Mariko Shinoyama, Noriko Takaya, Yuko Yamaguchi, Ryuta Kishii, Kazuhiko Iwase, Naoki Ando, Masahiro Nomura, and Yasushi Kohno

ACS Med. Chem. Lett., **Just Accepted Manuscript** • DOI: 10.1021/acsmedchemlett.6b00057 • Publication Date (Web): 05 Apr 2016

ACS Publications

ACS Medicinal Chemistry Letters is published by the American Chemical Society. 1155 Sixteenth Street N.W., Washington, DC 20036

LpxC Inhibitors: Design, Synthesis, and Biological Evaluation of Oxazolidinones as Gram-negative Antibacterial Agents

Haruaki Kurasaki*, Kosuke Tsuda, Mariko Shinoyama, Noriko Takaya, Yuko Yamaguchi, Ryuta Kishii, Kazuhiko Iwase, Naoki Ando, Masahiro Nomura, and Yasushi Kohno

Watarase Research Center, Kyorin Pharmaceutical Co., Ltd., 1848 Nogi, Nogi-machi, Shimotsuga-gun, Tochigi 329-0114, Japan

ABSTRACT: Herein we report a scaffold-hopping approach to identify a new scaffold with a zinc binding head group. Structural information was used to give novel oxazolidinone-based LpxC inhibitors. In particular, the most potent compound, **23j**, showed a low efflux ratio, nanomolar potencies against *E. coli* LpxC enzyme, and excellent antibacterial activity against *E. coli* and *K. pneumoniae*. Computational docking was used to predict the interaction between **23j** and *E. coli* LpxC, suggesting that the interactions with C207 and C63 contribute to the strong activity. These results provide new insights into the design of next-generation LpxC inhibitors.

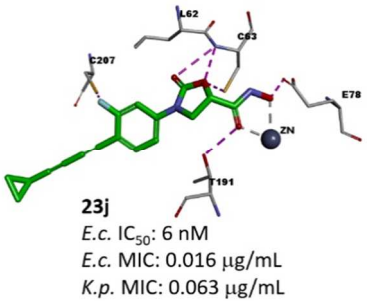

KEYWORDS: Antibacterial, Gram-negative bacteria, LpxC, scaffold hopping, oxazolidinone

In recent years, infections caused by antibiotic-resistant bacteria have emerged as major threats to human communities worldwide.[1] However, the late-stage clinical development pipeline for antibacterials has been unacceptably lean in recent decades.[2] In particular, no drugs have reached advanced stages of development for the treatment of infection due to multidrug-resistant Gram-negative bacteria. Thus, there is a great need to develop new mechanisms by which Gram-negative antibacterial agents can combat bacterial antibiotic resistance.[3,4]

One of the emerging targets in Gram-negative bacteria is LpxC, an essential enzyme in the lipid A biosynthetic pathway. Because LpxC does not show homology to any mammalian protein, it is a promising antibiotic target for developing novel therapeutics against multidrug-resistant Gram-negative pathogens.[5] LpxC inhibitors have drawn much attention in new entities for Gram-negative antibacterial agents.[6]

To date, extensive investigations have been carried out on the mechanism underlying the LpxC enzyme.[7,8] Those studies have identified a zinc ion to catalyze deacetylation and a hydrophobic tunnel binding a myristate fatty acyl chain of the natural substrate. Merck researchers discovered **1** (**L-161,240**) containing an oxazoline scaffold in the mid-1990s,[6] and recently several LpxC inhibitors have been reported as antibacterial agents,[9-17] although to our knowledge, none have reached the market yet.

Among the well-characterized compounds, threonyl-hydroxamate derivatives are representative LpxC inhibitors, such as **2** (**CHIR-090**) and **3** (**LPC-009**) (Figure 1 (a)).[18,19] According to a few reports on the binding modes of these compounds, the threonyl-hydroxamate group of **2** and that of **3** occupy the active site, and its diphenyl acetylene or phenyldiyne group penetrates the hydrophobic passage.[19-21]

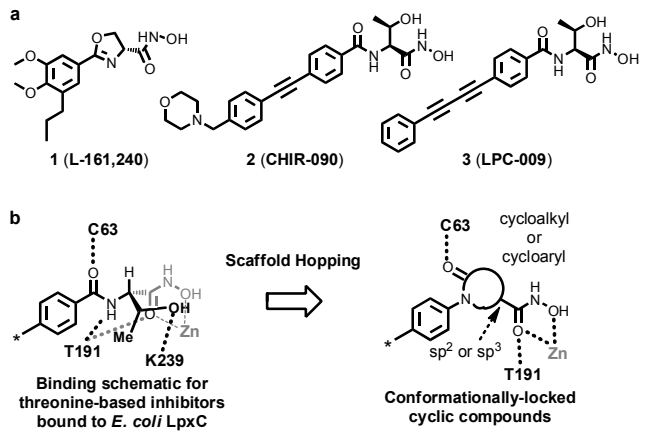

Figure 1. (a) Threonine-based LpxC inhibitors. (b) Scaffold hopping approach to LpxC inhibitors.

Scheme 1. Synthesis of Initially Designed Compounds[a]

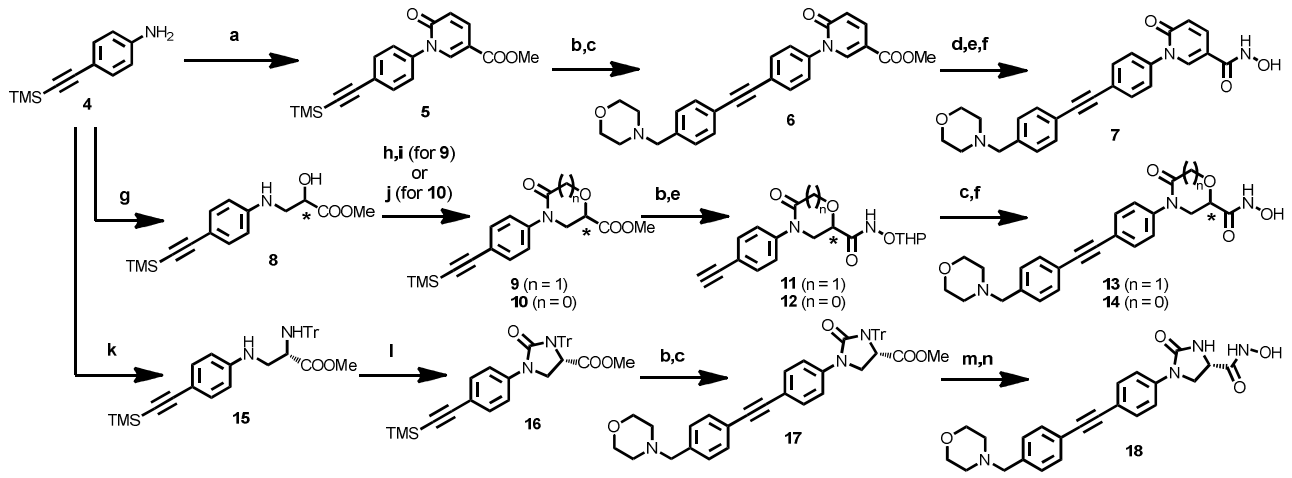

[a]Reagents and conditions: (a) 5-Methoxycarbonyl-2-pyrone, pyridine, 100 °C, 37%; (b) K_2CO_3, MeOH, rt, 86-96%; (c) 4-(4-Iodobenzyl)morpholine, $PdCl_2(PPh_3)_2$, CuI, Et_3N, THF, rt, 30-62%; (d) LiOH aq., THF/MeOH, rt; (e) $THPONH_2$, EDCI or HATU, *i*Pr_2NEt, DMF, rt; (f) 4 M HCl, dioxane/MeOH, rt, or TFA, CH_2Cl_2, rt, 46-61%; (g) Methyl (2*S*)-glycidate or methyl (2*R*)-glycidate, TfO-Li, CH_3CN, 60 °C, 34%; (h) Bromoacetylbromide, Et_3N, THF, rt; (i) NaH, THF, rt, 22% (2 steps); (j) CDI, CH_3CN, 60 °C, 46% (2 steps from **4**); (k) (*R*)-3-Oxo-(tritylamino)-propionic acid methyl ester, $NaBH(OAc)_3$, CH_2Cl_2, rt, 24%; (l) Triphosgene, Et_3N, CH_2Cl_2, rt, 82%; (m) HCOOH aq., THF 65 °C, 61%; (n) NH_2OH aq., *i*PrOH, rt, 80%.

Herein we report a scaffold hopping approach to identify a new scaffold with a zinc-binding head group. Additionally, we describe the synthesis, biological evaluation, and docking analysis of oxazolidinone-based LpxC inhibitors. Among these compounds, **23j** showed remarkable antibacterial activity.

In order to discover a novel scaffold to replace the threonine moiety, we embarked on a scaffold hopping approach utilizing structural information. The crystal structure and detailed analysis of the binding site for *E. coli* LpxC complexed with the threonine-based inhibitor **LPC-009** have been reported.[19,20] Inspection of the available co-crystal structures[20] indicated that the threonyl hydroxy group and benzamide moiety make key contacts with C63, T191, and K239 (left part in Figure 1 (b)). It is striking that the C=O bond of the benzamide and the C-H bond of threonyl α-methine lie in the same plane. We hypothesized that adjustment of the conformation of the amide and the hydroxamic acid makes better interactions with C63, T191, and zinc, thus makes it possible to improve activity even though the interaction with K239 is not available.[23] Therefore, we decided to incorporate the conformationally restricted cyclic moiety to retain the hydrogen-bonding network and overlapping with the positions of the central phenyl moiety and hydroxamic acid group of threonine-based inhibitors, as shown at right in Figure 1 (b).

A diphenyl acetylene hydrophobe, similar to **2** (**CHIR-090**), was chosen as a starting point for the initially designed compounds. The syntheses of these compounds are described in Scheme 1. All designed compounds were derived from 4-[(trimethylsilyl)ethynyl]aniline (**4**). Pyridone **5** was prepared by heating **4** with the corresponding pyrone in pyridine. For the preparation of the diphenyl acetylene unit, **5** was desilylated under basic conditions, followed by Sonogashira coupling with 4-(4-iodobenzyl)morpholine. Finally, methyl ester **6** was converted to the corresponding hydroxamic acid **7** in three steps: employing LiOH hydrolysis, coupling with *O*-THP-hydroxylamine, and acidic hydrolysis. A morpholin-3-one **9** or

Table 1. IC_{50} and MIC Values of Initial Compounds

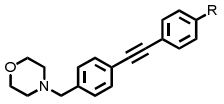

cpd	Structure R =	*E.c.* IC_{50} (nM)	MIC (μg/mL)		
			E.c.[a]	*E.c.*[b]	*K.p.*[c]
2	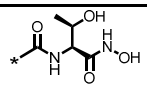	3	0.13	0.01	0.25
7	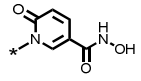	1000	8	1	64
(***S***)-**13**	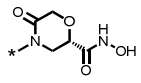	510	2	0.25	16
(***S***)-**14**	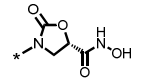	130	0.5	0.06	2
(***R***)-**14**	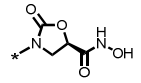	260	1	0.13	8
(***S***)-**18**	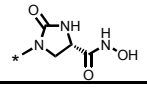	700	8	0.5	>32

[a]Wild-type *E. coli* TG1 strain. [b]Efflux mutant (*acrB*⁻) *E. coli* KAM3 strain. [c]Wild-type *K. pneumoniae* ATCC 13883 strain.

Scheme 2. Synthesis of Oxazolidinone-Based Diyne Compounds[a]

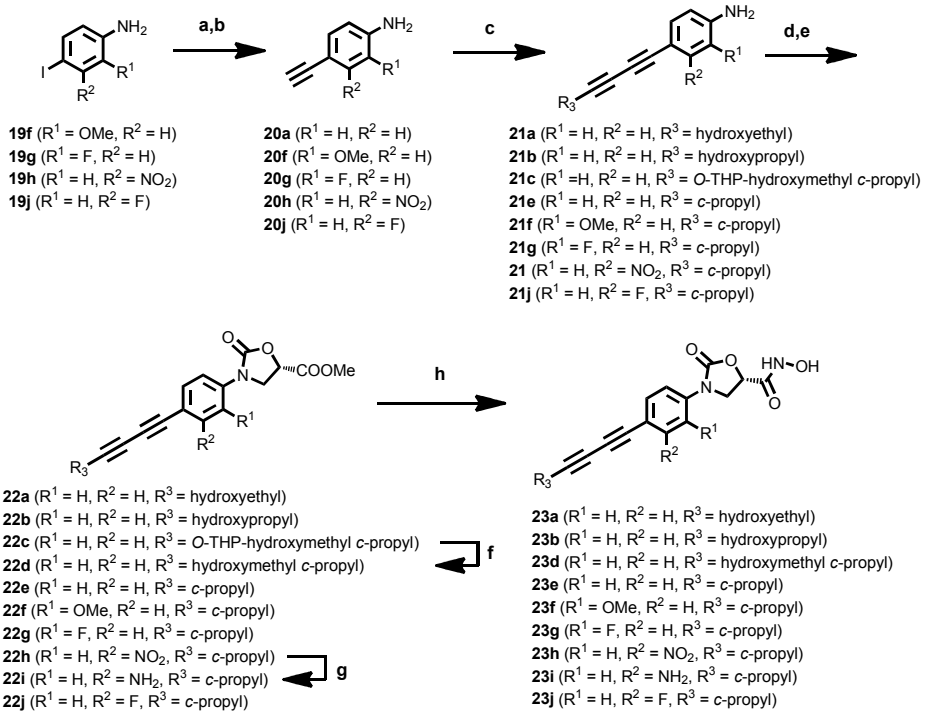

[a]Reagents and conditions: (a) TMS-acetylene, $PdCl_2(PPh_3)_2$, CuI, Et_3N, THF, rt; (b) K_2CO_3, MeOH, rt, 81-100% (2 steps); (c) Acetylene, $NiCl_2$ $6H_2O$, TMEDA, THF, rt, 24-73%; (d) Methyl (2*S*)-glycidate, TfOLi, CH_3CN, 60 °C; (e) i. CDI, CH_3CN, 60 °C, 16-56% (2 steps); ii. NaH, THF, 0 °C, 27% (3 steps) for only **22g**; (f) PPTS, MeOH, 50 °C, 77%; (g) Zn, AcOH, rt, 88%; (h) NH_2OH aq., *i*PrOH/THF, rt, 37-86%.

oxazolidinone **10** was formed by Lewis acid−induced epoxide ring opening using chiral methyl glycidate with **4**, followed by cyclization with bromoacetyl bromide or CDI. Meanwhile, for imidazolidinone, reductive alkylation of the corresponding aldehyde and **4**, followed the by the addition of triphosgene, affords **16**. Target compounds **13**, **14**, and **18** were afforded from **9**, **10**, and **16** in a similar manner as hydroxamic acid **7**.

Some of the newly designed compounds exhibited good cellular activity against *E. coli* and *K. pneumoniae*, although their activities in cell-free enzymatic assay were lower than that of **2** (Table 1). Pyridone **7** showed weak enzyme inhibitory activity and exhibited antibacterial activities with a minimum inhibitory concentration (MIC) of 8 μg/mL against an *E. coli* wild-type strain. Replacement of the pyridone moiety with the morpholine-3-one moiety improved IC_{50} value slightly and increased antibacterial activity 4-fold (compound **7** versus (*S*)-**13**). To our delight, ring compression to the oxazolidinone (*S*)-**14** resulted in much higher activity. Similar shifts in IC_{50} value in *E. coli* relative to the MIC values of *E. coli* and *K. pneumoniae* were observed (compound (*S*)-**13** versus (*S*)-**14**). Interestingly, (*S*)-**14** showed a good *E. coli* MIC value, although its enzyme activity was significantly lower than compared to that of **2**. At the same time, the absolute configuration in the 5-position of oxazolidinone was inverted from *S* to *R*. The activity of (*R*)-**14** was slightly lower than that of its *S*-enantiomer (2-fold shift in IC_{50} and MIC values). The substitution of oxazolidinone with imidazolidinone (*S*)-**18** led to the weakening of activity.

With oxazolidinone (*S*)-**14** in hand, we next varied the diphenyl acetylene moiety in order to evaluate the structure-activity relationship (SAR) of the hydrophobic group further. According to the reported co-crystal structures (3NZK[24] and 3P3G[20]), the terminal morpholine group of **2** and the phenyl group of **3** are surrounded by solvent-exposed lipophilic amino acid residues (M195, I198, Q202, S211, and F212) at the entrance to the hydrophobic passage. In particular, the terminal phenyl group of **3** forms an edge-to-face π−π interaction with F212.[19] These findings suggest that an sp^2-character-bearing moiety is suitable for interacting efficiently with F212.[18-21] Thus, we explored diyne compounds having various terminal functional groups. Moreover, we examined the SAR of the substitution effect on the central phenyl ring because we expected new interactions between the substituent and the amino acids positioned at the exit to the hydrophobic passage.[15]

The synthesis of oxazolidinone-based inhibitors with modified hydrophobes can be found in Scheme 2. The preparation of target compounds was initiated by Sonogashira reactions of 4-iodoaniline derivatives with TMS-acetylene followed by deprotection of the TMS group. A diacetylene unit was synthesized via Ni-catalyzed coupling reactions of terminal alkynes.[25] The desired hydroxamic acids were prepared in a manner similar to that described above.

The results of the oxazolidinone-based hydrophobe screening can be found in Table 2. Hydroxyethyldiyne **23a** retained

its activity, and the extension of the alkyl chain such as in **23b** showed a 3-fold increase in enzyme inhibitory activity and antibacterial activity. These results indicate that the terminal hydroxyl group was presumably located away from the hydrophobic passage. Potency increased slightly when the propyl group of **23b** was replaced by the methyl cyclopropyl group having an sp^2 character, such as in **23d**, which likely increased the hydrophobic interaction. Moreover, the removal of the hydroxymethyl group from **23d** increased *K. pneumoniae* antibacterial activity 4-fold, although the enzyme inhibitory activity was unchanged (**23e**).

Table 2. IC_{50} and MIC Values of Oxazolidinones

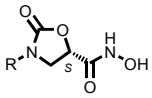

cpd	Structure R =	*E.c.* IC_{50} (nM)	MIC (μg/mL)		
			E.c.[a]	*E.c.*[b]	*K.p.*[c]
2		3	0.13	0.01	0.25
(*S*)-14		130	0.5	0.063	2
23a		140	0.5	0.125	8
23b		58	0.125	0.031	2
23d[d]		20	0.125	0.016	1
23e		18	0.063	0.016	0.25
23f		2000	4	0.5	32
23g		200	0.5	0.25	4
23h		270	0.25	0.063	2
23i		27	0.125	0.031	1
23j		6	0.016	0.004	0.063

[a]Wild-type *E. coli* TG1 strain. [b]Efflux mutant (*acrB*$^-$) *E. coli* KAM3 strain. [c]Wild-type *K. pneumoniae* ATCC 13883 strain. [d]Mixture of diastereomers.

Next we examined the SAR of the substitution effect on the central phenyl ring of **23e**. The introduction of a methoxy group at the *ortho*- position of the *N*-phenyl moiety resulted in a dramatic decrease in enzyme inhibitory activity, suggesting that dihedral restriction between phenyl and oxazolidinone due to the resonance and the steric effect of the methoxy group may be critical for the activity (compound **23e** versus **23f**). The fluorine-substituted **23g** was more active than **23f**, possibly because **23g** may have fewer dihedral restrictions (see Figure S2, Supporting Information). On the basis of these results, we next investigated substituent modification at the *meta*-position of the *N*-phenyl moiety, which we did not expect to appreciably affect the dihedral restrictions. The introduction of an electron-donating amino group to give **23h** significantly weakened enzyme inhibitory activity, whereas the strongly electron-withdrawing nitro group **23i** retained potency. Encouraged by this result, we introduced another electron-withdrawing and small lipophilic substituent. Changing NO_2 to F enhanced activity remarkably (*E. coli* MIC = 0.016 μg/mL and *K. pneumoniae* MIC = 0.063 μg/mL). As a result of this tuning of the hydrophobic group, **23j** was over 30-fold more potent than (*S*)-**14**. On the other hand, these new oxazolidiones had little or no effect against *Pseudomonas aeruginosa* and *Acinetobacter baumannii* (see Table S1, Supporting Information).

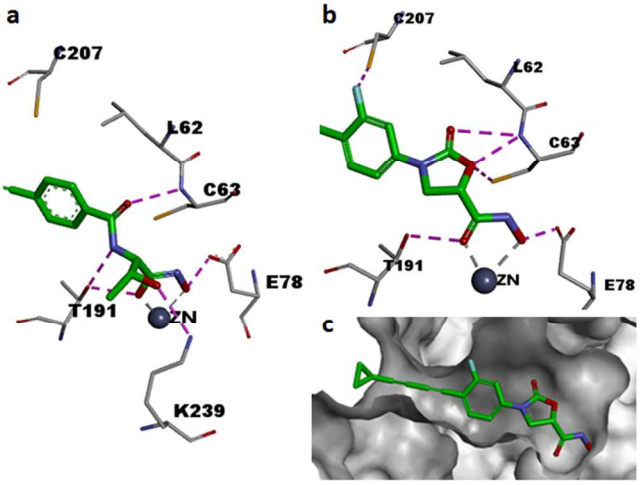

Figure 2. Comparative analysis of threonine-based and oxazolidinone-based inhibitors. (a) Threonine-based inhibitor **3** (**LPC-009**) bound co-crystal structure in *E. coli* LpxC (3P3G) showing key hydrogen bonds (pink dotted lines) and interaction with zinc (gray dotted lines).[20] (b)(c) Docking pose of **23j** bound to *E. coli* LpxC showing partially resected solvent-accessible surface (gray).

To examine the binding mode, we performed a docking study of **23j** to *E. coli* LpxC (Figure 2). The model clearly shows that the hydroxamic acid chelates the catalytic zinc ion with its two oxygen atoms. Additionally, it forms a hydrogen bond with T191 and E78, as in the case of **3** (**LPC-009**). On the other hand, the threonyl hydroxyl group of **3** forms a hydrogen bond with K239, but this interaction is not observed in the case of **23j**. As expected, the carbonyl oxygen atom of oxazolidinone is capable of accepting a hydrogen bond from the backbone NH of C63, corresponding to the oxygen atom in the benzamide moiety of **3**. Interestingly, the model indicates that the oxygen atom in position 1 of the oxazolidinone ring makes dual contacts with the backbone NH and the side chain thiol of C63. Also, it suggests that the fluorine atom on the phenyl group interacts with the thiol group of C207 (Figure 2 (b)(c)).[26] The fluorine atom contributes to the strong inhibition of enzymatic activity and antibacterial activity (compound **23e** versus **23j**). It appears that such additional interactions with C207 and C63, as in the case of **23j**, plays an important role in the remarkable activity enhancement without the key hydrogen-bonding interaction with K239, such as occurs in **3**. In general, oxazolidinone-based compounds can result in 2- to 8-fold lower efflux ratios (MIC value of wild-type strain/MIC

value of efflux knockout strain). The strong activity of **23j** against the *E. coli* wild-type strain contributes to the lower efflux ratio.

In summary, we conducted a scaffold hopping approach, which restricts the conformation of the threonine moiety, to discover a new series of LpxC inhibitors. We found oxazolidinone-based inhibitors. The most potent compound, **23j**, exhibited nanomolar potencies against *E. coli* LpxC enzyme, excellent antibacterial activity against *E. coli* and *K. pneumoniae*, and a low efflux ratio. Docking analysis of **23j** with *E. coli* LpxC suggested that the oxygen atom in position 1 of the oxazolidinone ring makes dual contacts with the backbone NH and the side chain thiol of C63 and the fluorine atom on the phenyl group interacts with the thiol group of C207. The interactions with C207 and C63 may contribute to the strong activity of **23j**. This observation provides new insights into the rational design of new LpxC inhibitors. These oxazolidinone-based inhibitors represent promising leads for further exploration as antibacterial agents.

ASSOCIATED CONTENT

Supporting Information

Synthetic method, characterization of compounds, protocols of biological evaluations, and computational methods. This material is available free of charge via the Internet at http://pubs.acs.org.

AUTHOR INFORMATION

Corresponding Author

*(H.K.) Tel: +81280571551; Fax: +81280572336; E-mail: haruaki.kurasaki@mb.kyorin-pharm.co.jp.

Author Contributions

All authors have approved of the final version of the manuscript.

Notes

The authors declare no competing financial interest.

ACKNOWLEDGMENT

We are thankful to H. Furuta of Kyorin Pharmaceutical Co., Ltd., for his mass spectrometry and infrared spectra expertise.

ABBREVIATIONS

LpxC, UDP-3-*O*-[(*R*)-3-hydroxymyristoyl]-*N*-acetylglucosamine deacetylase; *E.c., Escherichia coli*; *K.p., Klebsiella pneumoniae*; MIC, minimum inhibitory concentration; CDI, 1,1'-carbonyl diimidazole; TMS, trimethylsilyl; THP, tetrahydropyranyl; Tr, trityl; TMEDA, tetramethylethylenediamine; *c*-propyl, cyclopropyl; HATU, 1-[Bis(dimethylamino)methylene]-1H-1,2,3-triazolo[4,5-b]pyridinium 3-oxide hexafluorophosphate; EDCI, 1-Ethyl-3-(3-dimethylaminopropyl)carbodiimide; PPTS, pyridinium *p*-toluenesulfonate.

REFERENCES

(1) Boucher, H. W.; Talbot, G. H.; Bradley, J. S.; Edwards, J. E.; Gilbert, D.; Rice, L. B.; Scheld, M.; Spellberg, B.; Bartlett, J. Bad bugs, no drugs: no ESKAPE! An update from the Infectious Diseases Society of America. *Clin. Infect. Dis.* **2009**, *48*, 1-2.

(2) Devasahayam, G.; Scheld, W. M.; Hoffman, P. S. Newer antibacterial drugs for a new century. *Expert Opin. Invest. Drugs* **2010**, *19*, 215-234.

(3) Payne, D. J.; Gwynn, M. N.; Holmes, D. J.; Pompliano, D. L. Drugs for bad bugs: confronting the challenges of antibacterial discovery. *Nat. Rev. Drug Discovery* **2007**, *6*, 29-40.

(4) Silver, L. L. Challenges of antibacterial discovery. *Clin. Microbiol. Rev.* **2011**, *24*, 71-109.

(5) Young, K.; Silver, L. L.; Bramhill, D.; Cameron, P.; Eveland, S. S.; Raetz, C. R.; Hyland, S. A.; Anderson, M. S. The envA permeability/cell division gene of Escherichia coli encodes the second enzyme of lipid A biosynthesis. UDP-3-*O*-(*R*-3-hydroxymyristoyl)-*N*-acetylglucosamine deacetylase. *J. Biol. Chem.* **1995**, *270*, 30384-30391.

(6) Onishi, H. R.; Pelak, B. A.; Gerckens, L. S.; Silver, L. L.; Kahan, F. M.; Chen, M. H.; Patchett, A. A.; Galloway, S. M.; Hyland, S. A.; Anderson, M. S.; Raetz, C. R. Antibacterial agents that inhibit lipid A biosynthesis. *Science*, **1996**, *274*, 980-982.

(7) Coggins, B. E.; Li, X.; McClerren, A. L.; Hindsgaul, O.; Raetz, C. R.; Zhou, P. Structure of the LpxC deacetylase with a bound substrate-analog inhibitor. *Nature Structural Biology* **2003**, *10*, 645-651.

(8) Clayton, G. M.; Klein, D. J.; Rickert, K. W.; Patel, S. B.; Kornienko, M.; Zugay-Murphy, J.; Reid, J. C.; Tummala, S.; Sharma, S.; Singh, S. B.; Miesel, L.; Lumb, K. J.; Soisson, S. M. Structure of the bacterial deacetylase LpxC bound to the nucleotide reaction product reveals mechanisms of oxyanion stabilization and proton transfer. *J. Biol. Chem.* **2013**, *288*, 34073-34080.

(9) Mansoor, U. F.; Vitharana, D.; Reddy, P. A.; Daubaras, D. L.; McNicholas, P.; Orth, P.; Black, T.; Siddiqui, M. A. Design and synthesis of potent Gram-negative specific LpxC inhibitors. *Bioorg. Med. Chem. Lett.* **2011**, *21*, 1155-1161.

(10) Zhang, J.; Zhang, L.; Li, X.; Xu, W. UDP-3-*O*-(*R*-3-hydroxymyristoyl)-*N*-Acetylglucosamine deacetylase (LpxC) inhibitors: A new class of antibacterial agents. *Curr. Med. Chem.* **2012**, *19*, 2038-2050.

(11) Warmus, J. S.; Quinn, C. L.; Taylor, C.; Murphy, S. T.; Johnson, T. A.; Limberakis, C.; Ortwine, D.; Bronstein, J.; Pagano, P.; Knafels, J. D.; Lightle, S.; Mochalkin, I.; Brideau, R.; Podoll, T. Structure based design of an *in vivo* active hydroxamic acid inhibitor of *P. aeruginosa* LpxC. *Bioorg. Med. Chem. Lett.* **2012**, *22*, 2536-2543.

(12) McAllister, L.A.; Montgomery, J.I.; Abramite, J.A.; Reilly, U.; Brown, M.F.; Chen, J. M.; Barham, R.A.; Che, Y.; Chung, S.W.; Menard, C.A.; Mitton-Fry, M.; Mullins, L. M.; Noe, M. C.; O'Donnell, J. P.; Oliver, R. M. 3rd.; Penzien, J.B.; Plummer, M.; Price, L. M.; Shanmugasundaram, V.; Tomaras, A. P.; Uccello, D. P. Heterocyclic methylsulfone hydroxamic acid LpxC inhibitors as Gram-negative antibacterial agents. *Bioorg. Med. Chem. Lett.* **2012**, *22*, 6832-6838.

(13) Brown, M. F.; Reilly, U.; Abramite, J. A.; Arcari, J.T.; Oliver, R.; Barham, R. A.; Che, Y.; Chen, J. M.; Collantes, E. M.; Chung, S. W.; Desbonnet, C.; Doty, J.; Doroski, M.; Engtrakul, J. J.; Harris, T. M.; Huband, M.; Knafels, J. D.; Leach, K. L.; Liu, S.; Marfat, A.; Marra, A.; McElroy, E.; Melnick, M.; Menard, C. A.; Montgomery, J. I.; Mullins, L.; Noe, M. C.; O'Donnell, J.; Penzien, J.; Plummer, M. S.; Price, L. M.; Shanmugasundaram, V.; Thoma, C.; Uccello, D. P.; Warmus, J. S.; Wishka, D. G. Potent inhibitors of LpxC for the treatment of Gram-negative infections. *J. Med. Chem.* **2012**, *55*, 914-923

(14) Montgomery, J.I.; Brown, M.F.; Reilly, U.; Price, L. M.,; Abramite, J. A.; Arcari, J.; Barham, R.; Che, Y.; Chen, J. M.; Chung, S. W.; Collantes, E. M.; Desbonnet, C.; Doroski, M.; Doty, J.; Engtrakul, J. J.; Harris, T. M.; Huband, M.; Knafels, J. D.; Leach, K. L.; Liu, S.; Marfat, A.; McAllister, L.; McElroy, E.; Menard, C. A.; Mitton-Fry, M.; Mullins, L.; Noe, M. C.; O'Donnell, J.; Oliver, R.; Penzien, J.; Plummer, M.; Shanmugasundaram, V.; Thoma, C.; Tomaras, A. P.; Uccello, D. P.; Vaz, A.; Wishka, D. G. Pyridone methylsulfone hydroxamate LpxC inhibitors for the treatment of serious Gram-negative infections. *J. Med. Chem.* **2012**, *55*, 1662-1670.

(15) Hale, M. R.; Hill, P.; Lahiri, S.; Miller, M. D.; Ross, P.; Alm, R.; Gao, N.; Kutschke, A.; Johnstone, M.; Prince, B.; Thresher, J.; Yang, W. Exploring the UDP pocket of LpxC through amino acid analogs. *Bioorg. Med. Chem. Lett.* **2013**, *23*, 2362-2367.

(16) Murphy-Benenato, K. E.; Olivier, N.; Choy, A.; Ross, P. L.; Miller, M. D.; Thresher, J.; Gao, N. Hale, M. R. Synthesis, structure, and SAR of Tetrahydropyran-based LpxC inhibitors. *ACS Med. Chem. Lett.* **2014**, *5*, 1213-1218.

(17) Szermerski, M.; Melesina, J.; Wichapong, K.; Löppenberg, M.; Jose, J.; Sippl, W.; Holl, R. Synthesis, biological evaluation and molecular docking studies of benzyloxyacetohydroxamic acids as LpxC inhibitors. *Bioorg. Med. Chem.* **2014**, *22*, 1016-1028.

(18) Barb, A. W.; Jiang, L.; Raetz, C. R. H.; Zhou, P. Structure of the deacetylase LpxC bound to the antibiotic CHIR-090: Time-dependent inhibition and specificity in ligand binding. *Proc. Natl. Acad. Sci.* **2007**, *104*, 18433-18438.

(19) Liang, X.; Lee, C.-J.; Chen, X.; Chung, H. S.; Zeng, D.; Raetz, C. R. H.; Li, Y.; Zhou, P.; Toone, E. J. Syntheses, structures and antibiotic activities of LpxC inhibitors based on the diacetylene scaffold. *Bioorg. Med. Chem.* **2011**, *19*, 852-860.

(20) Lee, C.-J.; Liang, X.; Chen, X.; Zeng, D.; Joo, S. H.; Chung, H. S. Barb, A. W.; Swanson, S. M.; Nicholas, R. A.; Li, Y.; Toone, E. J.; Raetz, C. R. H.; Zhou, P. Species-specific and inhibitor-dependent conformations of LpxC: implications for antibiotic design. *Chemistry & Biology* **2011**, *18*, 38-47.

(21) Liang, X.; Lee, C.-J.; Zhao, J.; Toone, E. J.; Zhou, P. Synthesis, structure, and antibiotic activity of aryl-substituted LpxC inhibitors. *J. Med. Chem.* **2013**, *56*, 6954-6966.

(22) Lee, C. J.; Liang, X.; Gopalaswamy, R.; Najeeb, J.; Ark, E. D.; Toone, E. J.; Zhou, P. Structural basis of the promiscuous inhibitor susceptibility of Escherichia coli LpxC. *ACS Chem. Biol.* **2014**, *9*, 237-246.

(23) Sun, H.; Tawa, G.; Wallqvist, A. Classification of scaffold-hopping approaches. *Drug Discov. Today.* **2012**, *17*, 310-324.

(24) Cole, K. E.; Gattis, S. G.; Angell, H. D.; Fierke, C. A.; Christian, D. W. Structure of the metal-dependent deacetylase LpxC from Yersinia enterocolitica complexed with the potent inhibitor CHIR-090. *Biochemistry* **2011**, *50*, 258-265.

(25) Yin, W.; He, C.; Chen, M.; Zhang, H.; Lei, A. Nickel-catalyzed oxidative coupling reactions of two different terminal alkynes using O_2 as the oxidant at room temperature: facile syntheses of unsymmetric 1,3-diynes. *Org. Lett.* **2009**, *11*, 709–712.

(26) According to the docking pose, the F···HS distance is 1.63 Å and the F···SH distance is 2.60 Å. No further information is available on the type of interaction. Generally, fluorine is a considerably weaker hydrogen-bond acceptor than oxygen or nitrogen due to the very low polarizability of fluorine atoms and their tightly contracted lone pairs.[27] On the other hand, the latest PDB data suggest that fluorine is capable of forming halogen bonds with nitrogen and oxygen as well as sulfur.[28]

(27) Dunitz, J. D.; Taylor, R. Organic fluorine hardly ever accepts hydrogen bonds. *Chem. Eur. J.* **1997**, *3*, 89-98.

(28) Sirimulla, S.; Bailey, J. B.; Vegesna, R.; Narayan, M. Halogen interactions in protein-ligand complexes: Implications of halogen bonding for rational drug design. *J. Chem. Inf. Model.* **2013**, *53*, 2781-2791.

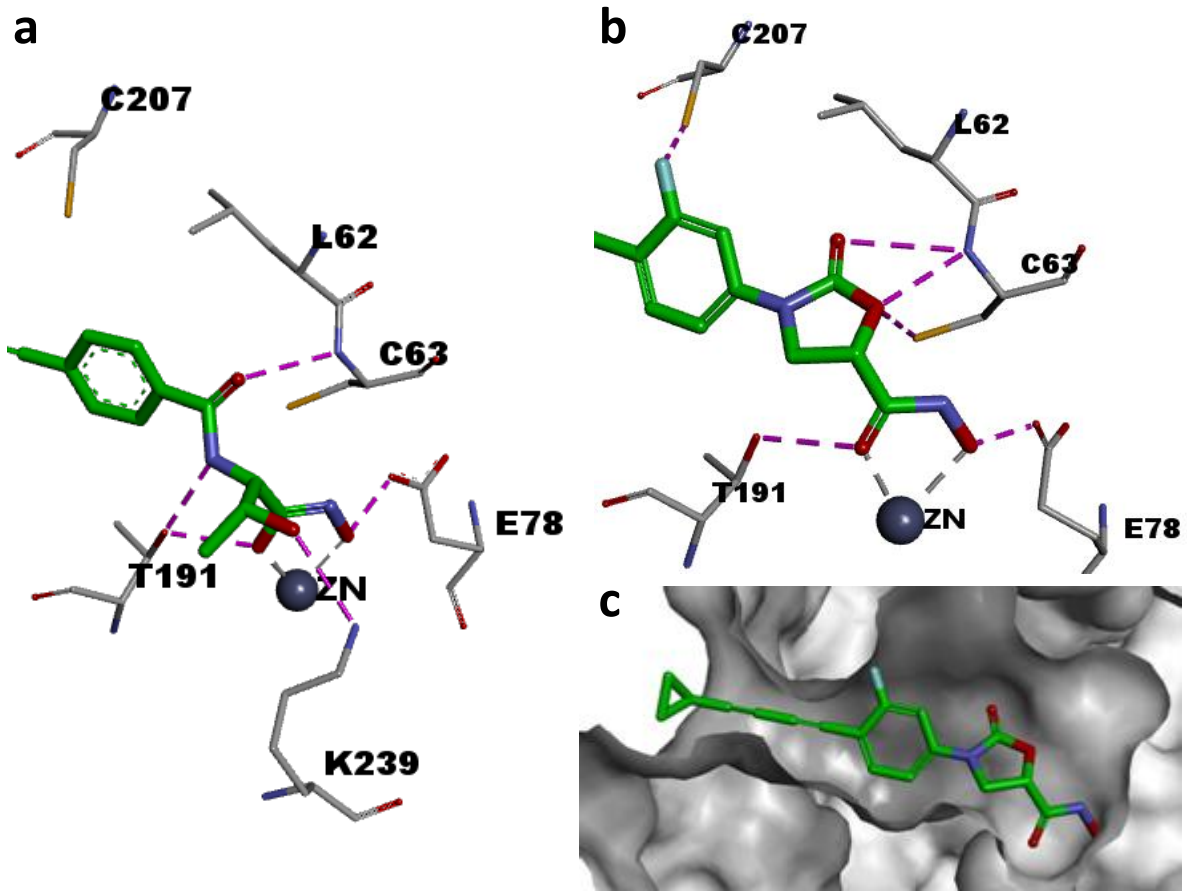
a
C207
L62
C63
E78
T191
ZN
K239
b
C207
L62
C63
T191
ZN
E78
c

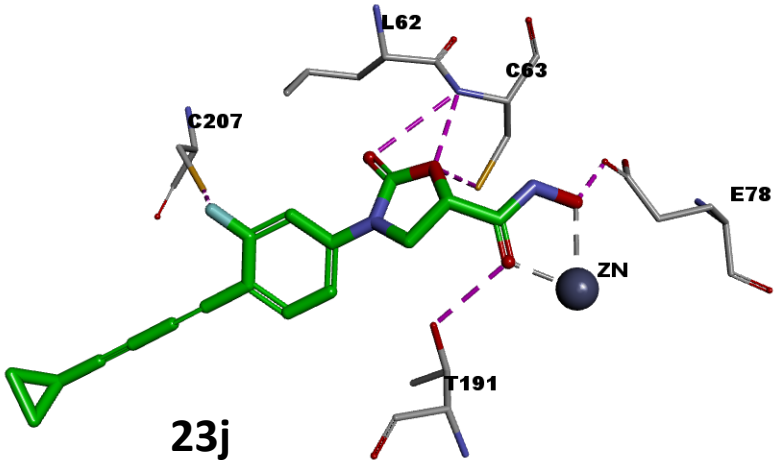

23j

E.c. IC_{50}: 6 nM

E.c. MIC: 0.016 μg/mL

K.p. MIC: 0.063 μg/mL